

Aromatic Oligoamide β -Sheet Foldamers

Laure Sebaoun,^{†,¶} Victor Maurizot,^{*,†,¶} Thierry Granier,^{†,¶} Brice Kauffmann,^{‡,¶,§} and Ivan Huc^{*,†,¶}

[†]Université de Bordeaux, CBMN (UMR 5248), Institut Européen de Chimie Biologie, 2 rue Escarpit, 33600 Pessac, France

[¶]CNRS, CBMN (UMR 5248), France

[‡]Université de Bordeaux, Institut Européen de Chimie Biologie (UMS 3033/US 001), 2 rue Escarpit, 33600 Pessac, France

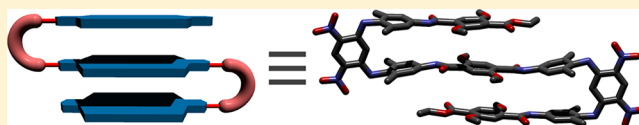
[#]CNRS, Institut Européen de Chimie Biologie (UMS 3033), 33600 Pessac, France

[§]INSERM, Institut Européen de Chimie Biologie (US 001), 33600 Pessac, France

Supporting Information

ABSTRACT: A rational approach for the construction of multi-stranded artificial β -sheets based not on hydrogen bonding, but rather on π - π aromatic stacking, is presented. Using 4,6-dinitro-1,3-phenylenediamine units, rigid turns were designed that allow face-to-face π - π interactions between

appended linear aromatic segments to be strong enough for folding in an organic solvent, but weak enough to prevent aggregation and precipitation. Solution and solid-state studies on a series of turn units showed that the desired degree of rigidity, resulting from hindered bond rotation, could be fine-tuned by the inclusion of additional methyl substituents on the aromatic rings. The high degree of preorganization afforded by these qualities further allowed the facile preparation of macrocyclic sheet structures from their noncyclic precursors. These macrocycles were shown to have slow internal dynamics and defined conformational preferences. Using this background, three- and five-stranded artificial β -sheets were synthesized and their folded conformations extensively characterized in solution by NMR. The solid-state structures of the three- and five-stranded sheets were also elucidated in the solid state by X-ray crystallography and confirmed intramolecular π - π aromatic stacking.



INTRODUCTION

The development of synthetic foldamers has thoroughly demonstrated that folded conformations do not belong solely to biopolymers but also occur in a wide variety of artificial oligomeric and polymeric backbones that can be remote from their natural counterparts.¹ Thus, a vast playground has been opened to chemists with the prospect to create artificial folded architectures with functions matching and exceeding those of peptides and nucleic acids. Remarkably, despite the variety of chemical units used to construct foldamers, a comparably narrow ensemble of secondary folded motifs has emerged. Apart from occasional unusual folded structures such as pillar-like architectures (stacks of aromatic rings),^{2,3} knots,⁴ spiral-like objects (“tail-biters”),⁵ a few zig-zag tapes,^{6,7} and non-canonical helices,⁸ a vast majority of foldamers are found to adopt the classical motifs found in biopolymers, namely helices, linear strands, turns and sheet-like structures, an observation that seems to have a theoretical basis.⁹ Among these secondary motifs, it is quite remarkable that foldamer helices are highly prevalent objects while artificial sheets are rare. A major difference between sheets and helices is that the latter fulfill their potential for non-covalent interactions intramolecularly giving rise to discrete and soluble structures, whereas the former tend to aggregate and precipitate. For example, natural peptidic β -sheets form stable finite well-defined structures in the context of protein tertiary folds, but polymerize into insoluble aggregates when in an isolated form. It follows that most artificial sheet-like structures possess features that prevent extensive aggregation. For instance, sheets based on inter-

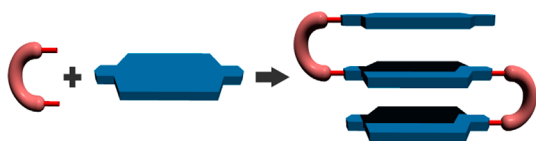
molecular hydrogen bonding are generally designed to be dimeric^{10–13} or monomeric,¹⁴ which ensures solubility. Otherwise, infinite assemblies may be observed.¹⁵ It is thus surmised that the rareness of foldamer sheets does not necessarily result from low occurrence, but from the fact that they may be difficult to track and remain undetected if not designed to be soluble. At the start of this investigation, rationally designed artificial sheets appeared to be elusive objects and their fabrication quite challenging.

In the following, we report the design, synthesis, and structural characterization of discrete, soluble β -sheet foldamers derived from aromatic oligoamides.¹⁶ Unlike in the few examples of artificial sheets and dimeric tapes mentioned above which rest on hydrogen bonding,^{10–13} the β -sheet foldamers presented here are stabilized by intramolecular aromatic π - π stacking. Relevant background to the development of these novel structures includes pillar-like architectures,^{2,3} some crescent-like macrocycles,¹⁷ foldamers with cofacial aromatic building blocks,¹⁸ zippers based on oligoantranilamides,¹⁹ and pyrrole–imidazole oligoamides that form stacked dimers upon binding to the minor groove of DNA,²⁰ as well as extensive work from our group on dimeric,²¹ trimeric,²² and tetrameric²³ β -helices, which can be viewed as strongly bent β -sheets that show the potential of aromatic oligoamides to assemble into discrete objects held by intermolecular aromatic π - π stacking.

Received: December 15, 2013

Published: January 14, 2014

Scheme 1. Schematic Assembly of the Design Elements for Building Aromatic Oligoamide β -Sheet Foldamers

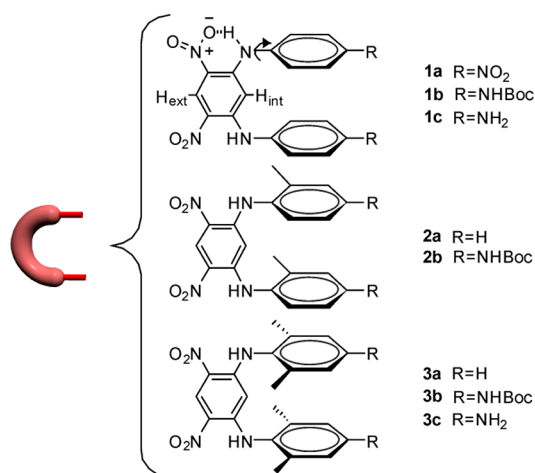


The design shown in Scheme 1 involves the combination of linear flat aromatic segments and of hairpin turns that would set the linear segments at a distance and orientation favoring aromatic stacking. A key parameter was to balance the strength of non-covalent interactions involved in folding and the level of pre-organization of the structure. On one hand, strong non-covalent interactions would be expected to result in folding but also in aggregation and precipitation as these interactions may occur in both intra- and intermolecular fashions. On the other hand, weak non-covalent interactions may not result in aggregation but may also fail to direct folding unless the structure is sufficiently preorganized. In the first generation of designs presented here, folding rests on aromatic stacking in chloroform, a solvent in which stacking is weakened by favorable solvent–solute interactions, and on an optimized turn unit that sets the orientation of aromatic groups so that intramolecular stacking results in multi-stranded sheet-like structures.

RESULTS AND DISCUSSION

Hairpin Turn Unit Design. Aliphatic three-atom spacers have been previously found to be suitable to connect two aryl rings and allow their face-to-face stacking, but only in the context of DNA minor groove binders.²⁰ To impart rigidity, sp^2 -conjugated spacers have also been used such as tertiary imides and ureas,³ 1,3-phenylene⁷ and 1,8-diphenyl-naphthalene¹⁸ groups. Among these, 4,6-dinitro-1,3-phenylenediamine possesses an attractive feature in that intramolecular hydrogen bonds between amine and nitro groups are expected to favor a parallel orientation of aromatic substituents (see compound **1**, Chart 1). However, previous examples of the use of this moiety in the context of arylamine oligomers showed that rotation about the amine–phenyl substituent bond resulted in reduced π – π overlap between phenyl rings.⁷ Only

Chart 1. Study of the Influence of Substituents of Adjacent Rings on the Folding of Pseudo- β -hairpins



in rigid macrocycles was the overlap found to be significant.²⁴ In order to limit this bond rotation, we investigated the effect of methyl groups *ortho* to the amine on the aryl substituents. Compounds **1**–**3** were prepared from 1,3-difluoro-4,6-dinitrobenzene via aromatic nucleophilic substitutions of the fluorine atoms by aromatic amines.²⁵ For **1b** and **1c**, the second substitution is slower than the first but both take place at room temperature. In contrast, heating to 80 °C is required for **1a** because of the poor nucleophilicity of the 4-nitroaniline precursor. In the case of the tolyl- and xylylamines involved to prepare compounds **2** and **3**, respectively, harsher conditions (80 °C) and long reaction times (10 days) are required for the second substitution to reach completion (see Supporting Information) due to the hindrance caused by the methyl groups.

¹H NMR spectra of **1b**, **2b**, and **3b**, which differ only by the number of methyl groups *ortho* to the diarylamine function, show little variations of the chemical shift value of H_{ext} , the proton *ortho* to both nitro groups that points toward the exterior of the structure ($\Delta\delta < 0.05$ ppm, see Figure 1A–C). In

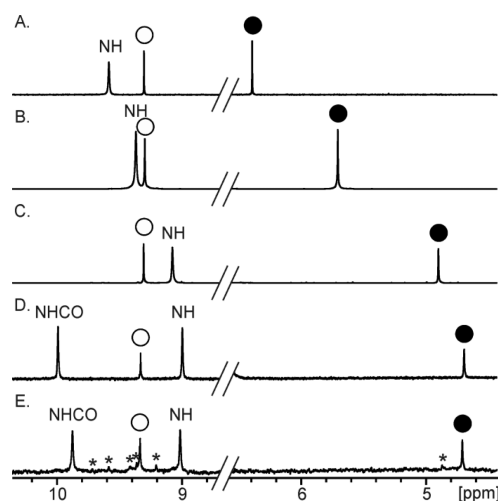


Figure 1. Parts of the 300 MHz ¹H NMR spectra in CDCl₃ at 298 K: (A) hairpin turn in the phenyl series **1b**; (B) hairpin turn in the tolyl series **2b**; (C) hairpin turn in the xylyl series **3b**; (D) OiBu macrocycle **5a**; and (E) OMe macrocycle **5b**. Signals of H_{ext} are marked with white circles. Signals of H_{int} are marked with full black circles. Stars indicate signals belonging to an impurity.

contrast, the resonance of H_{int} , the proton *meta* to both nitro groups that points toward the interior of the structure undergoes a major upfield shift of 1.5 ppm from **1b** to **3b**. This effect was assigned to the steric hindrance associated to the methyl groups that set the tolyl and even more so the xylyl rings in an orientation perpendicular to the dinitrophenyl unit, resulting in intense ring current effects over H_{int} . The xylyl series thus appears to provide a more rigid and better organized yet easy to prepare hairpin turn.

Further evidence of the effect of methyl groups was gathered in the solid state from the crystal structures of **1a**, **2a**, **2b**, **3a**, and **3b** (Figure 2). In the two distinct conformers found in the structure of **1a** and in the conformer of **2a** and of **2b** the phenyl or tolyl groups are not perpendicular to the dinitrophenyl unit, and not necessarily parallel to each other, leading to little π – π face-to-face overlap. On the contrary, the structures of **3a** and **3b** show well-organized conformations with parallel overlapping xylyl groups. The aryl–aryl distance between the xylyl

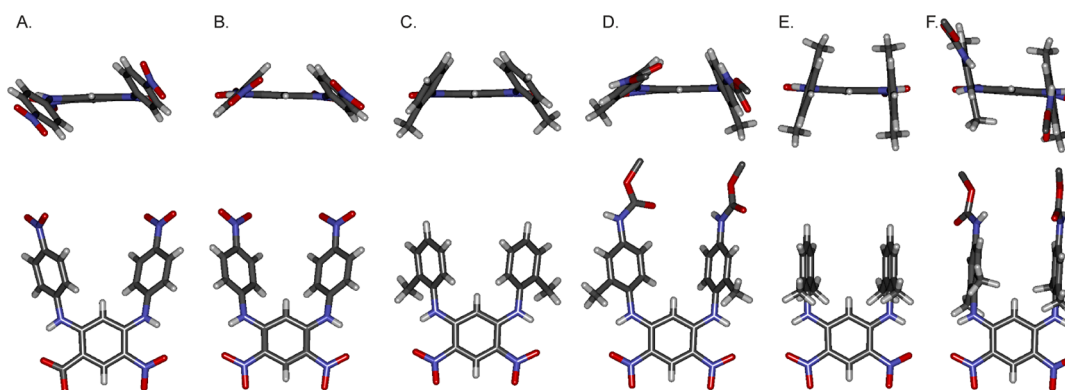
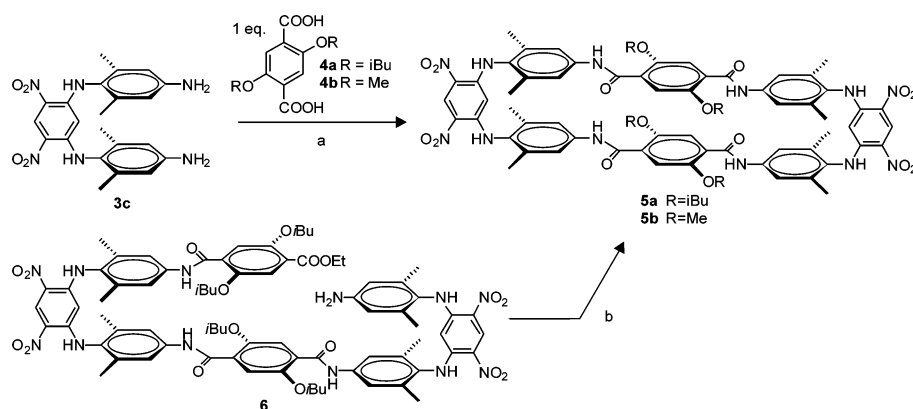


Figure 2. Side view (bottom) and front view (top) of the crystal structures: (A) form 1 of phenyl hairpin turn **1a**; (B) form 2 of phenyl hairpin turn **1a**; (C) tolyl hairpin turn **2a**; (D) tolyl hairpin turn **2b**; (E) xylyl hairpin turn **3a**; and (F) xylyl hairpin turn **3b**. Included solvent molecules and $-\text{CH}_3$ units of the Boc group in **2b** and **3b** have been omitted for clarity.

Scheme 2. Two Different Synthetic Pathways to Macrocycles **5a** and **5b**^a



^aReagents and conditions: (a) 6 equiv PyBOP, 6 equiv DIEA, CHCl_3 , 318 K, 7 days, 0.7 mM, yield for **5a** = 44%. (b) 5 equiv NaOH in THF/MeOH 2:1 v/v, 24 h, rt, then 3 equiv PyBOP, 3 equiv DIEA, CHCl_3 , 318 K, 7 days, 0.7 mM, yield for **5a** = 25%.

groups imparted by the dinitrobenzene unit is 4.8 Å, which is larger than desired for tight π - π contacts. Nevertheless, tight π - π contacts were found to take place upon elongation of the linear segments (see below) and the xylyl hairpin turn motif was selected to further develop β -sheet structures because of its well-controlled geometry.

Macrocyclic β -Sheets. For this proof-of-concept investigation, simple 2,5-dialkoxy-terephthalic acid units were selected to constitute linear segments connecting the hairpin turns (Scheme 1). The 2,5-alkoxy substituents provide hydrogen bond acceptors that favor coplanar orientation of the aryl and adjacent amide bonds following principles well established for other aromatic amide foldamers.¹⁶ Linear, tape-like, aromatic oligoamides have been described before²⁶ and may be envisaged to replace the terephthalic acid units and elongate the sheets in future designs. Crescent-shaped segments may be envisaged as well.^{17,27}

When allowed to polymerize, many aromatic oligoamide foldamer precursors have a high propensity to form macrocycles instead of long polymeric chains,^{28,29} as a consequence of the bent shape of short sequences imparted by folding. Prior to synthesizing long oligomers, we thus viewed the formation of macrocycles as a simple preliminary test of the folding propensity of our target sheet structures. Thus, diamino hairpin turn **3c** was reacted with 1 equiv of terephthalic acid having either 2,5-dimethoxy or 2,5-diisobutoxy substituents to produce 2+2 macrocycles (Scheme 2). Macrocycle **5a** was obtained in

44% (unoptimized) yield. Compound **5a** was also obtained in one coupling step from its linear precursor **6** (see below for the preparation of **6**). The production and purification of **5b** was complicated by its low solubility and only 7% of an enriched fraction was isolated.

A crystal structure of **6** clearly shows a C-shaped conformer in which the amine and ester functions, precursors of the cyclization step, are brought into close proximity by sheet-like folding (Figure 3A,B). A direct hydrogen bond was observed between the amine and ester carbonyl group ($d_{\text{N-O}} = 3.3$ Å). The distance between the terephthalic rings is 3.5 Å, as expected in aromatic stacks. In solution, this conformation is presumed to be at equilibrium with an S-shaped conformer in which the amine and ester functions are found on opposite sides of the central terephthalamide unit.

The low solubility of **5b** hampered its complete purification but was sufficient for ¹H NMR measurements in CDCl_3 . Compound **5a** was highly soluble. The spectra of **5a** and **5b** were compared to those of **3b** (Figure 1C–E). They showed an 0.2 ppm upfield shift of H_{int} with respect to **3b** which was interpreted as a further stabilization within the cyclic structure of a sheet-like conformation in which the linear segments are perpendicular to the dinitrophenyl turns, and H_{int} subjected to strong ring current effects from the xylylenediamine rings. Energy-minimized models of **5a** support this view (Figure 3D,F).

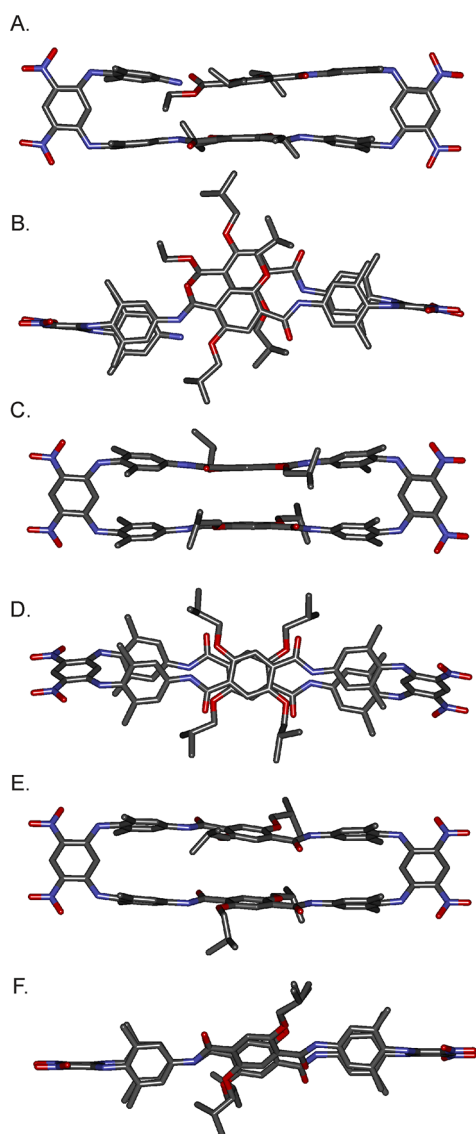


Figure 3. Side and top views of (A,B) the crystal structure of macrocycle precursor **6**; (C,D) the energy-minimized conformation (Maestro version 6.5 using the MM3 force field) of isobutoxy macrocycle **5a** as an anti-parallel conformer; and (E,F) the energy-minimized conformation of isobutoxy macrocycle **5a** as a parallel conformer. Both side and top representations were obtained by molecular modeling. Hydrogen atoms have been omitted for clarity.

The macrocycles thus represent rigid models of two-stranded sheets. They are nevertheless subject to internal dynamics. Indeed, xylylene aromatic protons H_3 and H_5 (Figure 4A) appear as a broad singlet at 7.44 ppm in the ^1H NMR spectrum of **5b**, and as two broad signals at 6.54 and 8.10 ppm in the spectrum of **5a** (Figure 4B,D). Upon heating, the two signals of the spectrum of **5a** coalesce; upon cooling to 273 K, these signals sharpen. In contrast, cooling a solution of **5b** results in a broadening of the signal at 7.44 ppm which eventually disappears into the baseline. Even at 223 K, its splitting into two signals was not observed.

The nonequivalence of H_3 and H_5 reflects the orientation of the central terephthalamide units with respect to the xylyl groups. One of the two xylyl protons is exposed to the amide carbonyl while the other faces the amide proton. Fast rotation of the xylyl units about themselves, or fast rotation of the

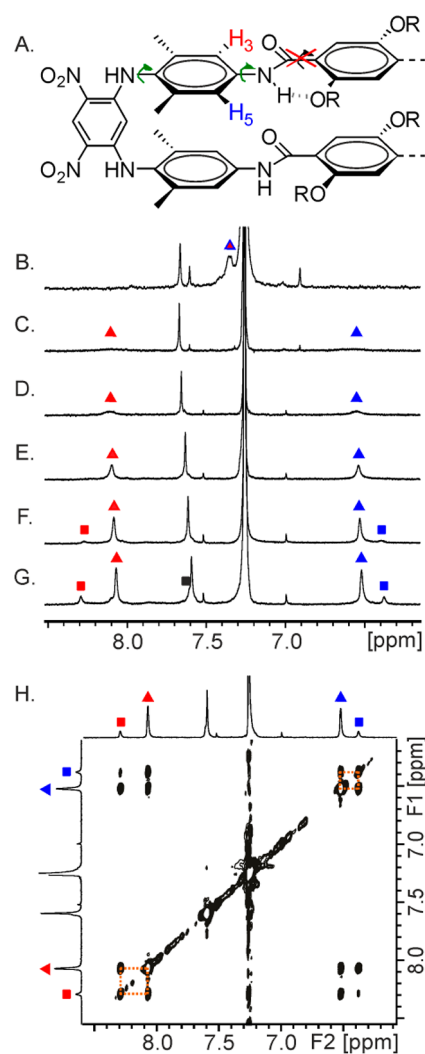
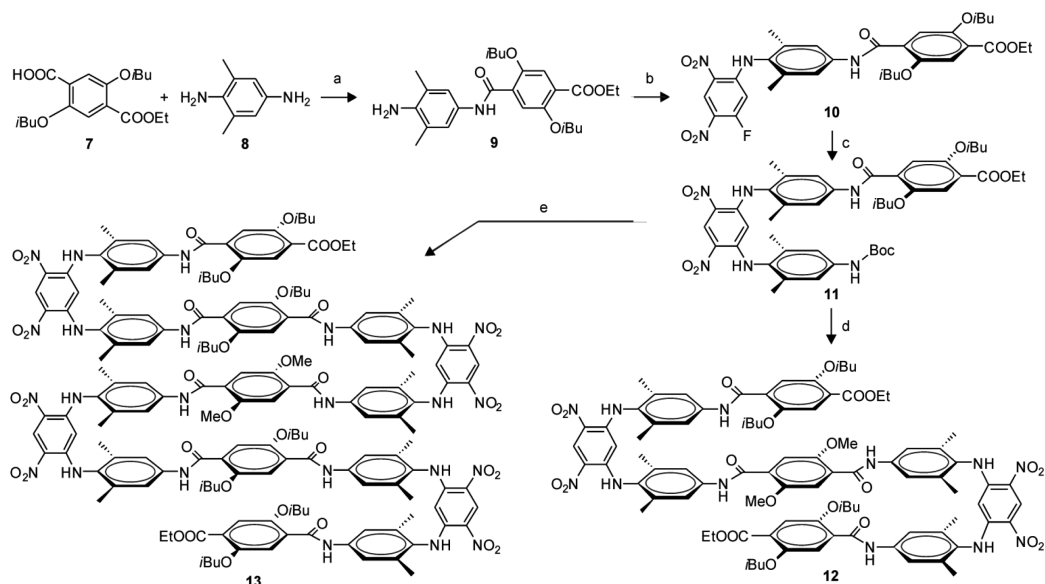


Figure 4. (A) Allowed rotations (green arrows) and rotation restricted by hydrogen bonding (red cross) of NH–aryl bonds in **5a** and **5b**; H_3 and H_5 are shown on the structure. (B–G) Parts of the 400 MHz ^1H NMR spectra in CDCl_3 of (B) **5b** at 298 K; (C) **5a** at 313 K; (D) **5a** at 298 K; (E) **5a** at 273 K; (F) **5a** at 248 K; and (G) **5a** at 223 K. H_3 and H_5 signals are marked with red and blue triangles, respectively. H_3+H_5 fast-exchange average signal is marked by a red-in-blue triangle. Signals belonging to a second conformer are marked with squares. (H) Excerpt of the 2D ROESY plot ($\tau_m = 300$ ms) at 223 K showing chemical exchange between protons of the two conformers of macrocycle **5a**.

terephthalamide units about themselves can in principle both result in equivalent H_3 and H_5 protons. The difference in behavior of **5a** and **5b** suggests that we are essentially observing a rotation of the terephthalamide units about themselves, and that the rotation of the xylyl units is a slower process. Rotation of the terephthalamides involves passing alkoxy substituents through the macrocycle cavity, a process that is expectedly much faster for the methoxy groups of **5b** than for the isobutoxy groups of **5a**. EXSY measurements on **5a** allowed the determination of a Gibbs energy of activation of 62 kJ/mol (see Supporting Information). No value could be calculated in the case of **5b**.

Upon cooling further a solution of **5a**, the signals of H_3 and H_5 broaden again and then both split into two signals of different intensities, indicating the presence of two distinct

Scheme 3. Synthesis of Multi-Turn β -Sheet Foldamers^a

^aReagents and conditions: (a) 1.2 equiv EDCl, CH₂Cl₂, 24 h, room temperature, yield = 82%. (b) 1 equiv 1,3-difluoro-4,6-dinitrobenzene, DMSO, 4 h, room temperature, yield = 95%. (c) 1 equiv *tert*-butyl-4-amino-3,5-dimethylphenylcarbamate, 1 equiv DIEA, DMSO, 353 K, 3 days, yield = 50%. For (d) and (e), see Supporting Information.

conformers in a ratio of 82:18 (Figure 4F,G). Exchange between these different signals is unambiguously confirmed by a 2D ROESY map (Figure 4H). This phenomenon was assigned to the coexistence of parallel and anti-parallel orientation of the central terephthalamide segments (compare panels D and F in Figure 3). Because of internal symmetry elements, each of these conformers possesses one type of H₃ proton, and one type of H₅ proton. The fast rotation of one terephthalamide unit amounts to fast equilibrium between the two conformers, but the complete coalescence of all H₃ and H₅ signals requires the fast rotation of both terephthalamide units. It is reasonable to hypothesize that the anti-parallel conformer is favored over the parallel conformer due to electrostatic effects, as is observed in the crystal structure of 6 (Figure 3A,B), thus reflecting direct interaction between the stacked aromatic rings.

Multi-Turn β -Sheet Structures. The stepwise synthesis of multi-turn sheets was carried out as outlined in Scheme 3 (see Supporting Information for more details). A convergent solution-phase approach was used, similar to that developed for helical oligomers.³⁰ Dimeric segment 9 could be prepared by selective coupling of the less hindered amine of xylylenediamine 8. Tetrameric building block 11 represents the repeat motif of the targeted sequences. It possesses a Boc-protected amine and a carboxylic acid protected as an ethyl ester. Deprotection of the amine of 11 and coupling with one terephthalic acid unit yielded nonameric three-stranded sheet 12. During this and other coupling steps, the diarylamine of 11 does not require any protection due to hindrance and its poor nucleophilicity. Similarly, an octamer (the Boc-protected analogue of octamer amine 6, see Scheme 2) was prepared from the free acid and the free amine derivatives of 11, and five-stranded heptadecamer 13 was assembled upon linking two octameric monoamines onto a terephthalic acid unit. For the purpose of facilitating NMR assignment, dimethoxy-terephthalamides were introduced in the central positions of 12 and 13 whereas diisobutoxy-terephthalamides were used at other

positions. Even the longest oligomer 13 was found to be well soluble (>8 mM) in chlorinated and aromatic solvents. The scheme was carried out on a 0.2 mmol scale but is in principle amenable to scaleup²⁹ and it may be applied to produce even longer structures.

The ¹H NMR spectra of tetramer 11, nonamer 12 and heptadecamer 13 are sharp and concentration independent and present no indication of aggregation. Upon increasing oligomer length, most signals undergo upfield shifts (Figure 5), H_{ext} being a notable exception. In particular, the signal of H_{int} in 11 and 12 were found at 4.87 and 4.85 ppm, respectively, values at slightly lower field than macrocycle 5a (4.70 ppm), whereas in 13, the two H_{int} protons were found at higher fields (4.69 and

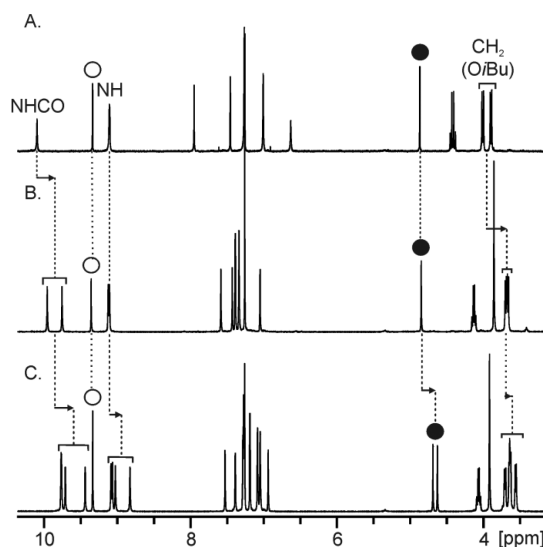


Figure 5. Parts of the 300 MHz ¹H NMR spectra in CDCl₃ at 298 K: (A) tetramer 11, (B) nonamer 12, and (C) heptadecamer 13. Signals of H_{ext} are marked with white circles. Signals of H_{int} are marked with full black circles.

4.63 ppm). This suggests a cooperative effect of the number of strands in the structure on its overall stability, due to cooperative interactions within aromatic stacks, resulting in enhanced ring current effects over H_{int} .

A series of multi-dimensional NMR experiments (HSQC, HMBC, TOCSY, and ROESY) allowed us to carry out the full assignment of the ^1H NMR spectra of **12** and **13**, and the assignment of the largest part of their ^{13}C NMR spectra. The protocols used for these assignments were similar to those described for helical aromatic oligoamides and critically involve short and long distance proton-carbon correlations.³¹ Both indirect and direct evidence of sheet-like folding in solution could be extracted from these data. For example, it was noticed that, when going from **12** to **13**, the largest upfield shifts concern the central xylyl protons ($\Delta\delta > 0.3$ ppm), a clear indication of their positioning at the center of the aromatic stack which expose them most to ring current effects. A large number of NOEs were observed that indicate multiturn sheet-like folding (see the Supporting Information): at every turn unit, the H_{int} proton correlate with the adjacent xylyl methyl protons; most importantly, the central methoxy protons correlate with aryl protons just above and below in the sheet. Nevertheless, the sheet-like structure appears to have much faster internal dynamics than macrocycle **5a** as far as rotations of the terephthalamide units about themselves are concerned. Even at low temperature, all signals remain sharp and no splitting of the xylyl protons were observed.

The multi-stranded sheet-like structures were further evidenced in the solid state by the crystal structures of both nonamer **12** and heptadecamer **13** (Figure 6) which show similar patterns. The three-stranded (two turns) conformation of **12** and five-stranded (four turns) conformation of **13** possess the expected shape, with the xylyl groups perpendicular to the dinitrophenyl moieties. The central part of each sheet consists of a face-to-face stack of three or five terephthalamide groups at a ca 3.5 Å distance for **12** and **13**, respectively, despite the fact that the aryl-aryl distance between the xylyl groups imparted by the dinitrobenzene unit is 4.8 Å, and thus reflecting attractive interactions between stacked linear segments. The terephthalamide rings are slightly offset from each other. This may correspond to more favorable π - π interactions.³² It may also reflect steric hindrance between isobutoxy side chains at the center of the sheets, or between nitro groups of dinitrophenyl moieties that come close in space upon folding. As in the structure of **6** (Figure 3A, 3B), adjacent terephthalamides are in an anti-parallel orientation in both **12** and **13**, supporting a more stable conformation of this arrangement, and again reflecting direct interactions between the stacked linear segments. These two structures suggest that the sheet motif may be elongated indefinitely, though elongation may require slight distortions as often observed in peptidic β -sheets which often adopt bent shapes.

CONCLUSION

We have introduced a rational approach for the construction of multi-stranded artificial β -sheets based not on hydrogen bonding, but rather on aromatic π - π stacking. Rigid turn units were designed that allow π - π interactions between linear aromatic segments to be strong enough for folding in organic solvents, but weak enough to prevent aggregation and precipitation. Structural investigation both in solution and in the solid state show that cyclic and non-cyclic oligomers adopt the expected sheet structures. The design principles reported

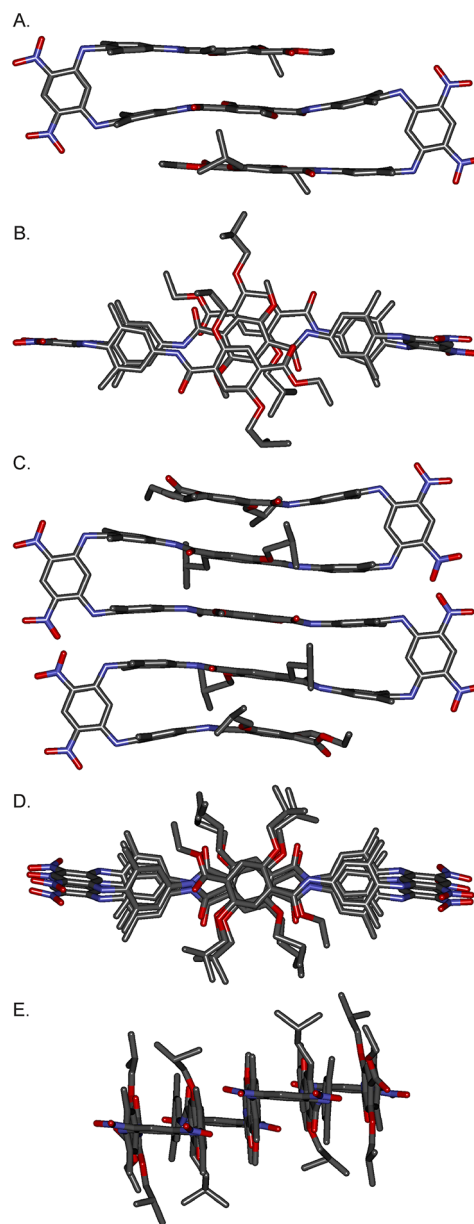


Figure 6. (A,B) Side and top views of the crystal structure of nonamer **12**. (C–E) Side, top, and front views of the crystal structure of heptadecamer **13**. Hydrogen atoms and included solvent molecules have been omitted for clarity.

here may be extended to a variety of patterns using diverse linear or bent segments connected by the turn units, giving rise to novel layered aromatic architectures of controlled size and shape. Research along these lines is currently in progress and will be reported in due course.

ASSOCIATED CONTENT

Supporting Information

Synthetic schemes, experimental procedures, full characterization of new compounds, crystallographic data, detailed NMR investigations including complete ^1H NMR assignment and solution structure elucidation of **12** and **13**. This material is available free of charge via the Internet at <http://pubs.acs.org>.

■ AUTHOR INFORMATION

Corresponding Authors

v.maurizot@u-bordeaux.fr

i.huc@iecb.u-bordeaux.fr

Notes

The authors declare no competing financial interest.

■ ACKNOWLEDGMENTS

This work was supported by the French Ministry of Research (predoctoral fellowship to L.S.) and by the European Research Council under the European Union's Seventh Framework Programme (Grant Agreement No. ERC-2012-AdG-320892). The authors thank Dr. Michael Singleton for proofreading the manuscript.

■ REFERENCES

- (1) For reviews, see: (a) Guichard, G.; Huc, I. *Chem. Commun.* **2011**, 47, 5933. (b) *Foldamers: Structure, Properties and Applications*; Hecht, S., Huc, I., Eds.; Wiley-VCH: Weinheim, 2007. (c) Goodman, C. M.; Choi, S.; Shandler, S.; DeGrado, W. F. *Nat. Chem. Biol.* **2007**, 3, 252. (2) (a) Bradford, V. J.; Iverson, B. L. *J. Am. Chem. Soc.* **2008**, 130, 1517. (b) Zych, A. J.; Iverson, B. L. *J. Am. Chem. Soc.* **2000**, 122, 8898. (c) Gabriel, G. J.; Sorey, S.; Iverson, B. L. *J. Am. Chem. Soc.* **2005**, 127, 2637. (d) Lokey, R. S.; Iverson, B. L. *Nature* **1995**, 375, 303. (3) (a) Tanatani, A.; Kagechika, H.; Azumaya, I.; Fukutomi, R.; Ito, Y.; Yamaguchi, K.; Shudo, K. *Tetrahedron Lett.* **1997**, 38, 4425. (b) Krebs, F. C.; Jørgensen, M. *J. Org. Chem.* **2002**, 67, 7511. (c) Masu, H.; Sakai, M.; Kishikawa, K.; Yamamoto, M.; Yamaguchi, K.; Kohmoto, S. *J. Org. Chem.* **2005**, 70, 1423. (4) Brüggemann, J.; Bitter, S.; Müller, S.; Müller, W. M.; Müller, U.; Maier, N. M.; Lindner, W.; Vögtle, F. *Angew. Chem., Int. Ed.* **2007**, 46, 254. (5) Hunter, C. A.; Spitaleri, A.; Tomas, S. *Chem. Commun.* **2005**, 3691. (6) (a) Prabhakaran, P.; Kale, S. S.; Puranik, V. G.; Rajamohanam, P. R.; Chetina, O.; Howard, J. A. K.; Hofmann, H.-J.; Sanjayan, G. J. *J. Am. Chem. Soc.* **2008**, 130, 17743. (b) Kendhale, A. M.; Gonnade, R.; Rajamohanam, P. R.; Hofmann, H.-J.; Sanjayan, G. J. *Chem. Commun.* **2008**, 2541. (7) (a) Maurizot, V.; Massip, S.; Léger, J.-M.; Délérès, G. *Chem. Commun.* **2009**, 5698. (b) Li, S.; Wang, D.-X.; Wang, M.-X. *Tetrahedron Lett.* **2012**, 53, 6426. (8) Delsuc, N.; Godde, F.; Kauffmann, B.; Léger, J.-M.; Huc, I. *J. Am. Chem. Soc.* **2007**, 129, 11348. (9) Chan, H. S.; Dill, K. A. *Annu. Rev. Biophys. Biophys. Chem.* **1991**, 20, 447. (10) (a) Nowick, J. S.; Chung, D. M.; Maitra, K.; Maitra, S.; Stigers, K. D.; Sun, Y. *J. Am. Chem. Soc.* **2000**, 122, 7654. (b) Nowick, J. S.; Brower, J. O. *J. Am. Chem. Soc.* **2003**, 125, 876. (c) Khakshoor, O.; Demeler, B.; Nowick, J. S. *J. Am. Chem. Soc.* **2007**, 129, 5558. (d) Khakshoor, O.; Lin, A. J.; Korman, T. P.; Sawaya, M. R.; Tsai, S. C.; Eisenberg, D.; Nowick, J. S. *J. Am. Chem. Soc.* **2010**, 132, 11622–11628. (e) Cheng, P.-N.; Pham, J. D.; Nowick, J. S. *J. Am. Chem. Soc.* **2013**, 135, 5477. (11) (a) Zhu, J.; Lin, J.-B.; Xu, Y.-X.; Shao, X.-B.; Jiang, X.-K.; Li, Z.-T. *J. Am. Chem. Soc.* **2006**, 128, 12307. (b) Xu, Y.-X.; Zhan, T.-G.; Zhao, X.; Li, Z.-T. *Org. Chem. Front.* **2014**, DOI: 10.1039/C3QO00032J. (12) (a) Gong, B.; Yan, Y.; Zeng, H.; Skrzypczak-Jankun, E.; Kim, Y. W.; Zhu, J.; Ickes, H. *J. Am. Chem. Soc.* **1999**, 121, S607. (b) Yang, X.; Martinovic, S.; Smith, R. D.; Gong, B. *J. Am. Chem. Soc.* **2003**, 125, 9932. (c) Gong, B. *Acc. Chem. Res.* **2012**, 45, 2077. (13) (a) Archer, E. A.; Sochia, A. E.; Krische, M. J. *Chem.—Eur. J.* **2001**, 7, 2059. (b) Archer, E. A.; Krische, M. J. *J. Am. Chem. Soc.* **2002**, 124, 5074. (c) Gong, H.; Krische, M. J. *J. Am. Chem. Soc.* **2005**, 127, 1719. (14) Wyrembak, P. N.; Hamilton, A. D. *J. Am. Chem. Soc.* **2009**, 131, 4566. (15) (a) Baruah, P. K.; Sreedevi, N. K.; Majumdar, B.; Pasricha, R.; Poddar, P.; Gonnade, R.; Ravindranathan, S.; Sanjayan, G. J. *Chem. Commun.* **2008**, 712. (b) Kendhale, A.; Gonnade, R.; Rajamohanam, P. R.; Sanjayan, G. J. *Chem. Commun.* **2006**, 2756. (16) For reviews about aromatic oligoamides foldamers, see: (a) Huc, I. *Eur. J. Org. Chem.* **2004**, 17. (b) Zhang, D.-W.; Zhao, X.; Hou, J. L.; Li, Z. T. *Chem. Rev.* **2012**, 112, 5271. (17) Lin, L.; Zhang, J.; Wu, X.; Liang, G.; He, L.; Gong, B. *Chem. Commun.* **2010**, 46, 7361. (18) Prabhakaran, P.; Puranik, V. G.; Chandran, J. N.; Rajamohanam, P. R.; Hofmann, H.-J.; Sanjayan, G. J. *Chem. Commun.* **2009**, 3446. (19) Nair, R. V.; Kheria, S.; Rayavarapu, S.; Kotmale, A. S.; Jagadeesh, B.; Gonnade, R. G.; Puranik, V. G.; Rajamohanam, P. R.; Sanjayan, G. J. *J. Am. Chem. Soc.* **2013**, 135, 11477. (20) (a) Mrksich, M.; Parks, M. E.; Dervan, P. *J. Am. Chem. Soc.* **1994**, 116, 7983. (b) Trauger, J. W.; Baird, E. E.; Dervan, P. B. *Nature* **1996**, 382, 559. (c) White, S.; Szweczyk, J. W.; Turner, J. M.; Baird, E. E.; Dervan, P. B. *Nature* **1998**, 391, 468. (d) Kielkopf, C. L.; White, S.; Szweczyk, J. W.; Turner, J. M.; Baird, E. E.; Dervan, P. B.; Rees, D. C. *Science* **1998**, 282, 111. (e) Hsu, C. F.; Phillips, J. W.; Trauger, J. W.; Farkas, M. E.; Belitsky, J. M.; Heckel, A.; Olenyuk, B. Z.; Puckett, J. W.; Wang, C. C.; Dervan, P. B. *Tetrahedron* **2007**, 63, 6146. (f) Li, B. C.; Montgomery, D. C.; Puckett, J. W.; Dervan, P. B. *J. Org. Chem.* **2013**, 78, 124. (21) (a) Berl, V.; Huc, I.; Khoury, R.; Krische, M. J.; Lehn, J.-M. *Nature* **2000**, 407, 720. (b) Berni, E.; Kauffmann, B.; Bao, C.; Lefeuvre, J.; Bassani, D. M.; Huc, I. *Chem.—Eur. J.* **2007**, 13, 8463. (c) Baptiste, B.; Zhu, J.; Haldar, D.; Kauffmann, B.; Léger, J.-M.; Huc, I. *Chem. Asian J.* **2010**, 5, 1364. (22) Ferrand, Y.; Kendhale, A. M.; Garric, J.; Kauffmann, B.; Huc, I. *Angew. Chem., Int. Ed.* **2010**, 49, 1778. (23) Gan, Q.; Bao, C.; Kauffmann, B.; Grélard, A.; Xiang, J.; Liu, S.; Huc, I.; Jiang, H. *Angew. Chem., Int. Ed.* **2008**, 47, 1715. (24) Bizier, N. P.; Vernamonti, J. P.; Katz, J. L. *Eur. J. Org. Chem.* **2012**, 2303. (25) (a) Touil, M.; Elhabiri, M.; Lachkar, M.; Siri, O. *Eur. J. Org. Chem.* **2011**, 10, 1914. (b) Hu, W.-J.; Ma, M.-L.; Zhao, X.-L.; Guo, F.; Mi, X.-Q.; Jiang, B.; Wen, K. *Tetrahedron* **2012**, 68, 6071. (26) (a) Hamuro, Y.; Geib, S. J.; Hamilton, A. D. *J. Am. Chem. Soc.* **1996**, 118, 7529. (b) Wu, Z.-Q.; Jiang, X.-K.; Zhu, S.-Z.; Li, Z.-T. *Org. Lett.* **2004**, 6, 229. (c) Odriozola, I.; Kyritsakas, N.; Lehn, J.-M. *Chem. Commun.* **2004**, 62. (27) Gong, B. *Chem.—Eur. J.* **2001**, 7, 4336. (28) Jiang, H.; Léger, J.-M.; Guionneau, P.; Huc, I. *Org. Lett.* **2004**, 6, 2985. (29) (a) Yamato, K.; Kline, M.; Gong, B. *Chem. Commun.* **2012**, 48, 12142. (b) Feng, W.; Yamato, K.; Yang, L.; Ferguson, J. S.; Zhong, L.; Zou, S.; Yuan, L.; Zeng, X. C.; Gong, B. *J. Am. Chem. Soc.* **2009**, 131, 2629. (30) Qi, T.; Deschrijver, T.; Huc, I. *Nat. Protoc.* **2013**, 8, 693. (31) Dolain, C.; Grélard, A.; Laguerre, M.; Jiang, H.; Maurizot, V.; Huc, I. *Chem.—Eur. J.* **2005**, 11, 6135. (32) Hunter, C. A.; Sanders, J. K. M. *J. Am. Chem. Soc.* **1990**, 112, 5525.